Anthropocene
March 2020, Volume 29, Pages 100230 (9p.)
https://doi.org/10.1016/j.ancene.2019.100230
https://archimer.ifremer.fr/doc/00593/70540/

Oceanic mercury concentrations on both sides of the Strait of Gibraltar decreased between 1989 and 2012

Cossa Daniel [1, 2, *], Knoery Joel [2], Boye Marie [3], Marusczak Nicolas [2], Thomas Bastien [2], Courau Philippe [4], Sprovieri Francesca [5]

[1] ISTerre, Université Grenoble Alpes, BP 53, F-38041, Grenoble, France
[2] IFREMER, Atlantic Center, LBCM, F-44031, Nantes, France
[3] Institut de Physique du Globe de Paris, Université de Paris, F-75238, Paris, France
[4] CNRS, LOV, F-06230, Villefranche-sur-Mer, France
[5] CNR, Institute of Atmospheric Pollution Research, I-87036, Rende, Italy

* Corresponding author : Daniel Cossa, email address : dcossa@ifremer.fr

Abstract :

Mercury (Hg) is a toxic metal that threatens the health of aquatic ecosystems and fish consumers. Its natural cycle has been deeply perturbed by Anthropogenic Hg emissions have deeply perturbed its natural cycle, especially since the start of the Industrial Revolution circa 1850 CE. Anthropogenic Hg emissions from North America and Europe have decreased by a factor of two in the last decades following the implementation of strict regulations. The response of North Atlantic Ocean and Mediterranean waters to this decrease remains poorly documented by field observations. A comparison of results obtained between 1989 and 2012 shows a significant decrease of Hg concentrations in waters on both sides of the Strait of Gibraltar. West of Gibraltar, the Hg decrease ranges from ~35 % in the upper North East Atlantic Deep Water to ~50 % in the North East Atlantic Central Water. East of Gibraltar, the observed decrease is ~30 % in the Western Mediterranean Deep Water. No decrease is observed in the deep Atlantic Ocean layer that formed before the industrial era. These results strongly substantiate the effectiveness of global anti-pollution policies on Hg contamination in oceanic waters. A consequent decline of Hg bioaccumulation in Northeastern Atlantic and Western Mediterranean pelagic ecosystems still requires verification.

Graphical abstract

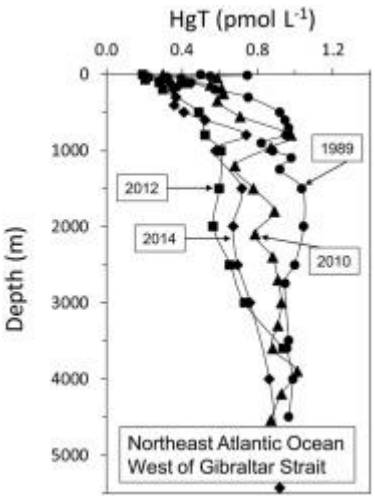

Highlights

► Hg concentrations in water columns have been determined both sides of the Gibraltar Strait ~20 years apart (1989–2012). ► The decrease range between ~30 and ~50 % in WMDW and NEACW, respectively. ► Hg concentrations did not change in the deepest waters of the Atlantic Ocean.

Keywords : Mercury, Mediterranean Sea, Atlantic Ocean, Gibraltar

Abbreviations

AABW: Antarctic Bottom Water

AOU: Apparent oxygen utilization

BrCl: Bromine monochloride

CFC's: Chlorofluorocarbons

CO: Carbon monoxide

CRM: Certified reference material

FEP: Fluorinated ethylene propylene

GEOTRACES: An international study of the marine biogeochemical cycles of trace elements and their isotopes (www.geotraces.org)

Hg: Mercury

Hg^0: Elemental mercury

HgR: Reactive or easily reduced mercury

HgT: Total mercury

HgTUNF: Total mercury in unfiltered samples

HgTF: Total mercury in filtered samples

LDW: Lower Deep Water

LIW: Levantine Intermediate Water

LSW: Labrador Sea Water

MeHg: Methyl mercury

MAW: Modified Atlantic Water

MW: Mediterranean Water

NEACW: North East Atlantic Central Water

NEADW: North East Atlantic Deep Water

O_3: Ozone

OFFTRAC: University of Washington three-dimensional offline ocean tracer model.

ORMS-4: Certified reference material (River water spiked with inorganic mercury).

P: Phosphorus

P_{rem}: Remineralized phosphorus

$SnCl_2$: Tin chloride

SPMW: Subpolar Mode Water

SRP: Soluble reactive phosphorus

US-EPA: Environmental Protection Agency of the United States of America

WIW: Winter Intermediate Water

WMDW: Western Mediterranean Deep Water

Keywords: *Mercury, Mediterranean Sea, Atlantic Ocean, Gibraltar*

1. Introduction

Mercury (Hg) is a trace element which affects human health primarily *via* marine fish consumption (e.g., Fitzgerald et al., 2007). Its toxicity is essentially due to the presence of methylmercury (MeHg), which biomagnifies up food webs (e.g., Clarkson and Magos, 2006). In aquatic environments, MeHg is formed by methylation of inorganic Hg by microorganisms (e.g., Jensen and Jernelöv, 1969; Parks et al., 2013). In the open ocean, although MeHg formation has been shown in sub-surface seawater and sediments (e.g., Monperrus et al., 2007; Hollweg et al., 2010; Soerensen et al., 2016), it occurs mainly in the

thermocline/intermediate waters (200-1000 m) where most bacterial organic matter regeneration occurs (e.g., Mason and Fitzgerald, 1990; Cossa et al., 2009; Blum et al., 2013; Cossa et al., 2017). Inorganic Hg reaches the thermocline/intermediate waters *via* the solubility and biological pumps (e.g., Fitzgerald and Lamborg, 2003; Mason et al., 2012; Lamborg et al., 2016; Semeniuk and Dastoor, 2017). The solubility pump advects Hg with water circulation, while the biological pump transports Hg to deep water with sinking biogenic debris after its adsorption/uptake by phytoplankton in the upper reaches of the water column. At thermocline/intermediate levels, inorganic Hg associated with particulate matter is partially dissolved during the remineralization of organic matter and used as a substrate by microorganisms for MeHg synthesis. Since direct atmospheric Hg deposition represents the principal source of inorganic Hg to the open ocean (e.g., Mason et al., 2012; Sonke et al., 2013), its rates of deposition and transport to thermocline/intermediate layer depths are, along with the intensity of microbial activity there, the primary control factors on Hg methylation. Ultimately, these parameters control the exposition of the base of the aquatic food web to MeHg levels and thus constrain human contamination from seafood resources.

The Hg natural biogeochemical cycle has been disrupted by human activities for several millennia (e.g., Cooke et al., 2009; Elbaz-Poulichet et al., 2011; Mason et al., 2012). According to Amos et al. (2013), simulations show that the present-day Hg concentration in the atmosphere is enriched by a factor of 2.6 relative to pre-industrial times (before ~1850 AD) and by a factor of 7.5 relative to natural levels. A recent critical review concludes that atmospheric Hg concentrations have risen by about 4.5 times above the level prevailing before 1450 AD (Outridge et al., 2018), and that this increase has driven a 3-fold increase in the average deposition rates to the Earth's surface, which in turn has elevated Hg levels in oceanic waters. Mass balance calculations suggest that within the last century Hg increased by ~200% in the surface ocean, ~25% in subsurface waters, and ~10% in recently formed

deep waters (Mason et al., 2012). Modelling oceanic Hg changes in the last millennium (Zhang et al., 2014a and b) suggests a Hg increase by a factor of 4.4 in the ocean mixed layer, whereas the inventory of Hg has increased by 50 and 20% in the thermocline/intermediate and deep ocean, respectively. Using a different approach, Lamborg et al. (2014a) calculated that Hg concentrations have increased by 250%, 160% and 10% in surface, thermocline/intermediate, and deep waters. They argue that these 3 layers contain respectively 6%, 59% and 35% of total oceanic anthropogenic Hg. These figures are comparable with the values of 3% in surface, 52% at thermocline/intermediate depths, and 45% for the deep ocean estimated by Zhang et al. (2014b). For their part, Outridge et al. (2018), in their updated global and oceanic Hg budget, suggest that the oceanic Hg concentrations increased compared to natural level by a factor of 2.3 in surface waters and by only 12-25% in deeper layers. In addition, global Hg emissions, as well as the deposition rates, are geographically heterogeneous, and the time-trends of Hg change in oceanic waters are consequently geographically dependent (Mason et al., 2012; Lamborg et al. 2014b). For example, the waters of the Pacific Ocean show a Hg increase at depths between 200 and 1000 m during the last few decades, while such a trend is not observed from measurements for North Atlantic waters (Mason et al., 2012). Irrespective of the uncertainties of these various estimates, all previously quoted studies converge in establishing that the anthropogenic emissions of Hg and subsequent oceanic loading have massively increased since the beginning of the industrial time. These anthropogenic perturbations will persist for years to centuries depending on the geographical position and oceanic layer concerned. An insight of the relative persistence of anthropogenic Hg can be derived from the residence times of Hg, which are roughly < 1 year in the mixed layer (Soerensen et al., 2010), ~120 years in the thermocline/intermediate layer, and ~2000 years in deep layers (Zhang et al., 2014b).

Observations in recent years of Hg concentrations in the atmosphere contrast with the long-term assessments. Indeed, the Hg concentrations in the troposphere of the northern hemisphere and the wet deposition have declined by ~35% during the 1990-2010 period (Prestbo and Gay, 2009; Slemr et al., 2011; Muntean et al., 2014). More specifically, a temporal decrease of Hg concentrations in the marine boundary layer of the North Atlantic atmosphere was observed during the same period (Sprovieri et al., 2010; Cole and Steffen, 2010; Mao and Talbot, 2012; Weigelt et al., 2014). Zhang et al. (2016) reviewing the recent atmospheric data conclude that the decrease in atmospheric elemental Hg (Hg^0) concentrations ranges from 1.2 to 2.1 percent per year at northern midlatitudes, and that wet deposition fluxes follow these trends. Similar observations for the oceanic waters are lacking due to the sheer difficulty in obtaining an adequately long time series of quality Hg concentration data (in both precision and accuracy) Hg concentration data. For an example, a set of four measurements, obtained between 1980 and 2010, tends to suggest that surface concentrations in the North Atlantic have decreased since the 1980s (Fig. 4 *in* Driscoll et al., 2013). These data are obviously limited in their ability to provide a basis for sound conclusions. For instance, the compilation of a larger dataset collected in the water column of the North Atlantic Ocean near Bermuda (Fig. 4b *in* Mason et al., 2012) conversely does not show a clear Hg decrease either at the surface or in intermediate or deep waters when early data (i.e., the samples collected in 1979 that may be poorly validated) are excluded. Mercury concentrations in the Eastern North Atlantic measured at the beginning of the 2000s (Cossa et al., 2004) and in 2014 during a GEOTRACES cruise (Cossa et al., 2018a) are difficult to compare because the data were obtained using different techniques for total Hg determination. Indeed, the former method (hydride formation) is different from the now validated bromine oxidation and tin chloride method (see Materials and Methods section) which is widely used and considered as *the* reference method by research programs and many

national and international agencies. Nevertheless, this comparison suggests a decrease in Hg concentration in the Mediterranean waters in recent decades, which has also been argued by Rajar et al. (2007) by using data partially obtained by the hydride technique (Cossa et al., 1997). Those decreases in the Mediterranean waters are consistent with the decrease of American and European Hg emissions (Streets et al., 2009; Pirrone et al., 2010). However, bearing in mind the uncertainty associated with the accuracy of early data, the observed decreasing trend and its magnitude is questionable. Despite these trends in marine waters being expected and predicted by modelling (Sunderland and Mason, 2007; Soerensen et al., 2012), they need to be confirmed by unambiguous field data acquired using consistent sampling and analytical techniques. Tentatively, a decrease by 30% in Hg concentrations is observed when using the same sampling procedure and analytical method in the North Atlantic (GEOTRACES GA-01 transect conducted in June 2014) between a recently formed core (1-3 years) of the Labrador Sea Water (LSW) and a core of LSW of 20 years old (Cossa et al. 2018a). Thus, additional field measurements are still clearly needed to actually observe and confirm the probable but still hypothetical decrease in Hg burden of the North Atlantic Ocean, both on a regional and seasonal basis. This latter is all the more important since biological pumping and net Hg deposition rates are geographically variable (Mason et al., 2012, 2017).

The Hg transfer at depth by biological pumping and Hg residence time at thermocline/intermediate layers of the global ocean (~120 years) suggest that these oceanic layers are the most suitable for investigating possible effects of changes in Hg deposition over scale of a century. In addition, the upper layers of the North Atlantic and the entire water column of the Western Mediterranean are also suitable water masses for studying decadal environmental changes, since their residence time are of the order of two decades (Cunningham, 2000; Béthoux et al., 2005, Schneider et al., 2014).

In this context, we are herein reporting the results of Hg determinations in the water column, obtained during oceanographic cruises conducted on both sides of the Strait of Gibraltar over the last 25 years using similar sampling and analytical techniques. The water column west of Gibraltar is included in the Subtropical North Atlantic Gyre (STG), which is one of the main features of North Atlantic circulation, and which anticyclonically links the Gulf Stream to the North Equatorial Current. The STG is a region where subtropical and recently ventilated waters mix, leading to an overturning of North Atlantic circulation (Carracedo Segade et al., 2015). The water column east of Gibraltar, the so-called Alboran Sea, contains the typical water masses of the Western Mediterranean (Millot et al., 2006; Garcia-Lafuente et al., 2017) characterized by high salinity values due to evaporation which exceeds precipitation reaching its maximum, particularly during summer. The Alboran Sea constitutes the reservoir of Mediterranean outflow to the North Atlantic through the Strait of Gibraltar. The objective of our study is answering the question: whether or not the decrease in atmospheric Hg concentrations at northern midlatitudes, at the turn of the century, has had a measurable impact on the Hg content of the water column of Northeast Atlantic and Western Mediterranean both sides of the Strait of Gibraltar. We show that a significant decrease in Hg concentrations occurs, between 1989 and 2012, in the upper and intermediate oceanic waters on both sides of the Strait of Gibraltar.

2. Material and Methods

Samples were collected during three different cruises, MEDATLANTE-II in September 1989, ALMOFRONT-I in May 1991, and FENICE in August 2012. The first two cruises were on board the French research vessel "Jean Charcot" and the FENICE cruise was on board the Italian research vessel "Urania" of the CNR (National Research Council). Two stations were

occupied west of Gibraltar: Sta. 6A during the MEDATLANTE-II cruise and Sta. 6B during the FENICE cruise (Fig. 1). Three stations were occupied in the Alboran Sea: Stas. 36, 63 and 65 during the ALMOFRONT-I cruise, and Stas. 4 and 8 during the FENICE cruise.

Water samples were collected using the most state-of-the-art techniques for ultra-trace Hg sampling and analysis that were available at the time of the cruises (Gill and Fitzgerald, 1985; Cossa and Courau, 1990; Mason and Fitzgerald, 1993; Yoon et al., 1996; Lamborg et al., 2012). During ALMOFRONT-I and MEDATLANTE-II cruises, stainless-steel rosette frame and hydrowire were deployed with acid-cleaned, Teflon-coated Go-Flo bottles (General Oceanics), whereas, during FENICE cruise, Niskin bottles (General Oceanics) placed on an epoxy-coated rosette and hung on a stainless steel hydrowire were used. During all three cruises, the rosettes were equipped with sensors for salinity, temperature, dissolved oxygen, and optical transmission. Samples for HgT determinations were treated and measured on board from sub-samples, using identical procedures in clean lab-vans (Class 100000-ISO8 equipped with Class 100-ISO5 laminar flow hoods). Samples were withdrawn from sampling bottles into acid-cleaned Teflon bottles (FEP), then stored acidified (Ultrapur HCl, 0.4% v/v) until analysis, which was always performed within the next 12 hours. In order to determine operationally defined total mercury (HgT) in the sample, Hg was released from its ligands and alkyl moieties through oxidation with BrCl. Dissolved, oxidized Hg was reduced to its Hg vapor with an acidic $SnCl_2$ solution. This technique, initially proposed by Bloom and Crecelius (1983), is now known as the US-EPA standard method N° 1631 (EPA, 2002). For our analyses, the Hg vapor is purged using Ar and amalgamated on a gold trap, then released by thermal desorption into an atomic fluorescence spectrometer (Merlin, PSA in 1989-91, and Tekran, Model 2500 in 2012). The detailed procedure for 1989-91 analyses is given by Courau (1983), and by Cossa et al. (2018b) for 2012 analyses. The differences between cruises are the following: in 1989-91, 125 mL of seawater sample was oxidized with the

bromide present in the seawater by the addition of 0.25 mL of a 0.04 mol L^{-1} potassium permanganate solution, then the Hg was reduced with 1 mL of a 0.05 M $SnCl_2$ solution. In 2012, the 100mL seawater subsample was oxidized with the addition of 0.1 mL of a 0.2 M BrCl solution, and Hg reduction was achieved by 0.2 mL of a 1 M $SnCl_2$ solution. The detection limit, defined at three times the standard deviation of six blank measurements, was 0.2 pmol L^{-1} and 0.1 pmol L^{-1} in 1989-91 and 2012, respectively. The reproducibility, defined as the coefficient of variation of six replicate samples, was 15% in 1989-91, and 12% in 2012. In 2012, the accuracy of Hg measurements was verified using the ORMS-4 certified reference material (CRM) from the National Research Council of Canada. Our measurements were always within the confidence limits given for the CRM. No CRM was commercially available at the time of MEDATLANTE-II and ALMOFRONT-I cruises, but accuracy was checked using two independent Hg standard solutions. Easily-reducible Hg (often called "reactive Hg", HgR) was also systematically measured on board. The data, not reported here, allowed the calculation of the mean HgR/HgT ratio, which was used to estimate the six missing HgT values (see SI 1). The quality of the analytical measurements was ensured by the use of the cleaning procedures for sampling and sample treatment that are recommended by Gill and Fitzgerald (1985), Mason and Fitzgerald (1993) and more recently by the GEOTRACES program, and by the rapidity of the onboard determinations after sampling. The capability of the two laboratories (LOV-CNRS and IFREMER) for producing high-quality ultra-trace measurements is shown by the results of their participation in most of the Hg intercomparison exercises for the aquatic environments over the last 25 years (e.g., Cossa and Courau, 1990; Lamborg et al., 2012).

3. Results and Discussion

3.1. Water masses and biogeochemical context

West of Gibraltar, temperature and salinity distributions at Sta. 6A (1989) and Sta. 6B (2012) are given in SI (Fig. S1a and b). The temperature *versus* salinity (T-S) graphs (Fig. 2) allow the same water masses to be identified during the two cruises; the presence of these water masses is well documented in this STG region (e.g., Pérez et al., 2018). Listing them from surface to bottom: (i) the surface (mixed) layer, (ii) the North East Atlantic Central Water (NEACW), (iii) the North East Atlantic Deep Water (NEADW) and (iv), at the bottom, the Lower Deep Water (LDW). The NEACW in the STG is composed of different mode waters including Mediterranean Water (MW) and Subpolar Mode Waters (SPMW), which both are clearly identified on the T-S graph in Figure 2 by high and low salinities, respectively (McCartney, 1992; Tsuchiya et al., 1992). The presence of MW is clearly identified by the salinity maximum located between 800 and 1250 m (SI, Fig. S1). The salinity variations along the Sta. 6A profiles testify to the presence of MW escaping the Strait of Gibraltar. Salinity (herein S*p*) is defined using the practical salinity scale from rosette sensor data. Using salinity of 35.5 and 38.5 S*p* for the Atlantic and Mediterranean end-members, the proportions of MW at Sta. 6A varied around 25% in 1989 (MEDATLANTE-II cruise). According to Yoon et al. (1996), who described zinc distribution from the same cruise, the salinity maximum (36.37 S*p*) corresponded to 32% of MW. At Sta. 6B occupied during the FENICE cruise (2012), the MW proportion reached 28% at the salinity maximum. There, the NEADW is underlain by the bottom layer constituted by LDW, which is a warmed Antarctic Bottom Water (AABW) coming from the Southern Ocean (Fig. 2). This deepest water mass contains very low chlorofluorocarbon (CFC's) concentrations, which attest for its pre-industrial atmospheric imprint (Rhein et al., 2002) and a Hg inventory attributable to the Hg solubility pump. During the MEDATLANTE-II cruise (1989), the soluble reactive phosphorus (SRP) distribution varied from 0.01 to 1.23 µmol L^{-1} between the surface and 2000 m. The

vertical profiles exhibited the typical pattern for this region with concentrations increasing rapidly from surface to 500-600 m, then decreasing slightly. The MW was located between 800 and 1200 m (SI, Fig. S2a). At deeper depths, SRP concentrations continued to increase at slower rates. During the FENICE cruise, at Sta. 6B, nutrient concentrations were not measured. As a proxy for SRP, we use remineralized phosphate (P_{rem}) calculated from the Apparent Oxygen Utilization (AOU) divided by a 141 Redfield ratio (Minster and Boulahdid, 1987), suggesting P_{rem} varied from 0.49 to 1.22 µmol L^{-1}. The concentration range and shape of the vertical profiles (SI, Fig. S2b) were similar during both the 1989 and 2012 cruises, suggesting that the biogeochemical conditions affecting Hg remobilization remained relatively unchanged during the 1989-2012 period.

In the Western Mediterranean Sea, the following water masses are from top to bottom: the modified Atlantic waters (MAW), the Levantine Intermediate Water (LIW), the Winter Intermediate Water (WIW), and the Western Mediterranean Deep Water (WMDW) (Millot et al., 2006; Garcia-Lafuente et al., 2017). The LIW, identified by a salinity maximum, is formed in the Eastern Mediterranean basin, while the WIW, identified by a temperature minimum, is formed along the continental shelf of the North Western Mediterranean basin. Finally, the WMDW is both the densest and coldest water present in the basin. The hydrological structures found during the ALMOFRONT-I (1991) and FENICE (2012) cruises were typical of the Alboran Sea (Tintoré et al., 1988; Béthoux et al., 2005). In addition, the ALMOFRONT-I conditions were given in detail by Prieur and Sournia (1994), who described the multiple-gyres and frontal structures. Station 4 (2012) was located in the Western Alboran cyclonic gyre, whereas Stas. 7 (2012) and 36 (1991) were located eastward in the Almeria cyclonic gyre, and Stas. 63 and 65 (1991) in the Cartagena anticyclonic eddy. Potential temperature *versus* salinity (T_p-S) graphs are given in Fig. 3, and T_p and salinity profiles in Fig. S3 (SI). The inflowing Atlantic water was located between 0 and 25 m depth with an

average S < 37 S*p*, and MAW was identified down to 100 m (S = 37-38 S*p*). The WIW (S = 38.2-38.3 S*p*) was found below 125 m down to the maximum of salinity at around 400 m, which characterized the LIW. The WMDW was located below 900 m depth (S = 38.42 S*p*). During the FENICE cruise, the T-S graph of Stas. 4 and 7 exhibited the same hydrological structure with the presence of MAW, WIW-LIW, and WMDW. In addition, surface temperatures of 18-25 °C showed the extension of summer surface stratification (FENICE cruise) that was not observed in spring (ALMOFRONT-I cruise). In the Alboran Sea, phosphorus concentrations varied from low values in surface waters to P_{rem} of 0.5 µmol L^{-1} in 1991. In 2012, P_{rem} also reached 0.6 µmol L^{-1} in deep waters. Vertical dissolved phosphorus profiles are shown (Fig. S4, SI). The P_{rem} data obtained in 2012 (FENICE cruise) were calculated from the AOU divided by a factor of 237, the specific Redfield ratio for the Western Mediterranean due to the P limitation of this oceanic region (Béthoux et al., 2005).

3.2. Mercury distributions

West of Gibraltar, in the Eastern North Atlantic, HgT concentrations measured in 1989 (Sta. 6A) varied from 0.21 to 1.07 pmol L^{-1} (Fig. 4). They ranged from 0.21 to 0.75 pmol L^{-1} in the surface layer, and increased from 0.21 at 40 m to ~1 pmol L^{-1} at 500 m within the SPMW, characterized by low temperature and salinity, and by peaking phosphorus levels (Fig. S1 and S2, SI). Below this depth, the profile showed a small Hg peak between 1000 and 1200 m. This relative maximum corresponds to the water layer (open circles in Fig. 4) where high salinity and low nutrients indicate the highest proportion of MW (Fig. SI, S1). Below 1200 m, the HgT levels were relatively less variable and ranged between 0.95 and 1.07 pmol L^{-1} in the NEADW and LDW. In comparison, HgT concentrations measured in 2012 (Sta. 6B) varied within a similar range, from 0.19 to 0.95 pmol L^{-1}. However, the concentrations were clearly lower in the NEACW (Fig. 4). The presence of MW at ~1000 m comes with a small inflexion in the HgT profile (open circles in Fig. 4). At greater depths (>3000 m), HgT

concentrations, obtained in 1989 and 2012, were converging to a mean value of 0.96 ± 0.04 pmol L^{-1} reached within the LDW. Since LDW results from the mixing of AABW with North Atlantic Deep waters during its northward transit, its relatively high mean HgT concentration is consistent with the elevated concentrations found recently (2014) in the lower NEADW during the GEOTRACES GA-01 transect (1.04 ± 0.02 pmol L^{-1} according to Cossa et al., 2018a) and at the source of AABW in the Southern Ocean in 2008 (1.35 ± 0.31 pmol L^{-1}) (Cossa et al., 2011). It can be surprising that, at depth as deep as 2500 m, HgT concentrations may have changed in a 20-years period. West of Gibraltar, NEADW spread down to 3000 m (Fig. 4). According to García-Ibáñez (2015), the water mass present at 3000 m is composed of 50-60% of LDW (called by these authors "lower-NEADW" or NEADWL) and similar proportions (20-25%) of LSW (Labrador Sea water) and ISOW (Island Scotland Outflow water). With a ventilation age of more than 150 years, NEADWL cannot contain recent anthropogenic Hg from the solubility pump. Conversely, LSW and ISOW, which are younger than 20 years (Doney et al., 1997), may have undergone changes in the Hg incorporation within the 1989-2012 period. Furthermore, in the layer of NEADW between 3000 and 2500 m the proportion of NEADWL is decreasing to 40% and at 2000 m it is less than 20%, whereas, parallelly, the proportion of the younger LSW is increasing up to 60%. Thus, a HgT change down to 2500-3000 m, at this place of the Northeast Atlantic Ocean within the 1989-2012 period, is rational.

East of Gibraltar, in the Alboran Sea (Fig. 1), HgT concentrations measured in 1991 varied from 1.28 to 2.44 pmol L^{-1} in the MAW, with an average of 1.71 pmol L^{-1}. They reached values higher than 2 pmol L^{-1} in the WIW, and averaged 1.42 and 1.32 pmol L^{-1} in the LIW and WMDW, respectively (Fig. 5). On the other hand, HgT concentrations measured in 2012 were clearly lower for the same water masses (0.33 to 0.96 pmol L^{-1}). Interestingly and in contrast to 1991, the lowest values in the subsurface waters were associated with the MAW probably as results of photoreduction and evaporation of Hg volatile species, whereas the highest were observed at depth (Fig. 5).

3.3. Time trends in Hg concentrations

Simple calculations can be done to estimate the temporal decrease of HgT concentration from direct comparison of the vertical profiles obtained in 1989, 1991 and 2012 (Figs. 4 and 5). West of Gibraltar, the amplitude of the Hg decrease diminished with depth. It ranges from ~50% in SPMW/NEACW to ~40% in MW/NEACW and ~35% in the upper NEADW. This last estimate is consistently similar to the 30% decline of Hg mean concentration observed in the core of LSW during the last 20 years (Cossa et al., 2018a). Below, in the aged LDW, no HgT change seems to have occurred between 1989 and 2012. East of Gibraltar, the observed decrease is ~30% in the herein sampled WMDW.

Another way to estimate the Hg decrease in the last 20 years that may reveal changes in the biogeochemical context, is to look at changes in the Hg/nutrient ratios. Indeed, Hg is thought to exhibit a nutrient-like behaviour in the North Atlantic Ocean (Cossa et al., 2004 and 2018a; Lamborg et al., 2014b; Bowman et al., 2015). This is confirmed by the statistically significant correlations between Hg and SPR or P_{rem} concentrations in both the 1989 and 2012 cruises west of Gibraltar (R^2 = 0.94 and 0.92, respectively, Fig. 6a). The regression coefficient calculated with 2012 data from Sta. 6B is 0.87 $\mu mol_{Hg}/mol_P$ based on an AOU/P_{rem} of 141 (Minster and Boulahdid, 1987), and it is 1.05 $\mu mol_{Hg}/mol_P$ if AOU/P_{rem} is 171 according to Lamborg et al. (2014b). This latter value is similar to that obtained for oceanic water not suspected of containing anthropogenic Hg, namely 1.02 ± 0.03 $\mu mol_{Hg}/mol_P$ (Lamborg et al., 2014b). The regression slope obtained in 1989 was lower (0.57 $\mu mol_{Hg}/mol_P$ based on an AOU/P_{rem} of 141, or 0.69 $\mu mol_{Hg}/mol_P$ if AOU/P_{rem} is 171) reflecting Hg-enrichment in P-poor surface water (Fig. 6a). According to the Lamborg et al. (2014b) model, this enrichment would be due to anthropogenic Hg since a "pristine relationship" is characterized by the global relationship for the World Ocean of $Hg_{[pmol\ L^{-1}]} = 1.01*P_{rem[\mu mol\ L^{-1}]} - 0.07$ (see discussion in the *Supplementary Information* section in Lamborg

et al.'s paper). The nutrient-like behavior of Hg means that a large fraction of surface Hg is drawn down to the ocean interior by sinking particles, where it is released as a result of organic matter microbiological remineralization, according to the well-known biological pumping/regeneration process (Sigman and Haug, 2006). East of Gibraltar, during the FENICE cruise in 2012, the Hg *versus* P_{rem} relationships were also statistically significant (R^2 = 0.95 and 0.76 at Stas 4 and 7, respectively, Fig. 6b). In contrast, during the ALMOFRONT-I cruise in 1991, the absence of a significant Hg *versus* SRP relationship (Fig. 6b) illustrated the fact that the major Hg enrichment at Stas. 63-65 was especially elevated in surface waters (Fig. 5). Normalized to common P concentrations, the Hg concentration decrease between 1991 and 2012 in the east of Gibraltar ranges ~38% for WMDW (for P = 0.6 µmol L^{-1}). West of Gibraltar, the P-normalized Hg decrease between 1989 and 2012 is ~30% at 1000 m (for P = 1.2 µmol L^{-1}) (i.e., in the MW/NEACW) increasing up to >50% in the subsurface water (i.e., upper SPMW/NEACW) (for P = 0.6 µmol L^{-1}).

It is interesting to note the contrasting situation which exists for deep waters east and west of Gibraltar. In the Alboran Sea, the Hg decrease is 30-38% in ~20 years old WMDW (Bethoux et al., 2005; Schneider et al., 2014), whereas, on the Atlantic side of Gibraltar Strait, the HgT concentration did not vary in the LDW between 1989 and 2012 (Fig. 4). This is entirely consistent with the pre-industrial age of these deepest oceanic waters. Furthermore, the Hg decrease between1989 and 2012 west of Gibraltar appears to be smaller for the oldest waters (NEADW) than that for younger ones (SPMW/NEACW). This result is consistent with the smaller decrease (30%) of the anthropogenic Hg fraction modeled in the deep waters of the North Atlantic at 35°N compared to that modeled at shallower depths (70%) (e.g., OFFTRAC-GEOS-Chem model; Zhang et al., 2014b). A minor part of the temporal decline in Hg concentrations in the intermediate waters of the North Atlantic between 1989 and 2012 might be attributed to the reduced efficiency of the biological pump, since the oceanic

primary production of North and Central Atlantic has slightly (-7%) decreased since the early1980s (Gregg et al., 2003). The dramatic drop of Hg concentrations actually observed in intermediate waters likely reflects the reduction in Hg deposition over the North Atlantic region over time (Soerensen et al., 2012; Weigelt et al., 2014). Indeed, this trend follows the temporal decline in Hg emission inventories for the Eastern United States of America since the mid-1990's years (Zhang et al., 2014b). Such decrease has already been observed in the North Western Atlantic near Bermuda but in sub-surface waters (Mason et al., 2012; Lamborg et al., 2014b). Additionally, recent Hg measurements performed in the water column of the North Eastern Atlantic in 2010 (GA-03 section) and 2014 (GA-01 section) (Fig. 4; Bowman et al., 2015; Cossa et al., 2018a) indicate, together with our dataset, that Hg concentrations have been declining between 1989 (Sta. 6A), 2010 (e.g., 0.68-0.89 pmol L^{-1} at Sta. 5) and 2012 (Sta. 6B) in the core of NEADW. Conversely, no significant decrease is observed between 2012 (Sta. 6B) and 2014 (Sta. 13), since HgT concentration ranges and distribution at depth were similar at both years (Fig. 4).

In the Alboran Sea, sources of Hg are (i) Atlantic waters inflowing the Mediterranean in surface, (ii) direct atmospheric deposition, and (iii) WIW, LIW and WMDW from the Western Mediterranean at depth. As discussed above, the Atlantic surface waters, sampled west of Gibraltar, show a decline in their Hg content (>50%) between 1989 and 2012. Thus, the influx of Hg from the Atlantic toward the Mediterranean is weakening with time. In addition, Alboran Sea waters are influenced by riverine metal sources (the mine-contaminated Tinto-Odiel-Huelva riverine system) inflowing the Gulf of Cadiz (van Geen et al., 1991). In the case of Hg, the concentrations were elevated in those rivers (up to 330 pmol L^{-1} in the Odiel River), and in the surface waters of the Gulf of Cadiz, the average dissolved Hg concentration was 2.9 ± 0.9 pmol L^{-1} in 1997-98 (Cossa et al., 2001). In 2012, during the 2012 FENICE cruise, dissolved Hg concentrations in the Gulf of Cadiz averaged only 0.55 ±

0.17 pmol L^{-1} (Knoery, unpublished). This decrease in Hg content in the Gulf of Cadiz surface waters may have contributed to the Hg decrease in the MAW entering the Alboran Sea. The direct Hg atmospheric deposition on the Alboran Sea has not been estimated. However, an atmospheric record of CO, O_3 and Hg across the Western Mediterranean and the Northeastern Atlantic (April 2012) indicates an Hg peak in the troposphere at Gibraltar, probably due to the densification of maritime traffic and industrialization at the Strait (Marusczak et al., unpublished, Fig. S5, SI). At depth, the Hg concentrations in WMDW have been found to be enriched during the winter water convection occurring in the Gulf of Lions and the adjacent gyre (Cossa et al., 2018b). The efficiency of the convection, which governs the Hg export at depth and its further exportation to the adjacent Northeast Atlantic, is variable from year to year, driven by the intensity of winter cooling of surface water (Marty and Chiaverini, 2010; Heimbürger et al., 2013; Macias et al., 2018). Furthermore, the Hg export to the Atlantic (i.e., the "Hg clearing rate" of the Mediterranean Sea) may have increased since the vertical export flux capacity seems to have increased since 1999 (Marty and Chiaverini, 2010).

Conclusions

Our work reveals that the decrease in atmospheric Hg concentrations, observed at the turn of the century in northern mid-latitudes, has had a measurable impact on the Hg content of oceanic waters. We showed that, using identical sampling and analytical techniques during four oceanographic cruises on both sides of the Strait of Gibraltar, Hg concentrations have significantly decreased between 1989 and 2012. West of Gibraltar, the Hg decrease ranges from ~35% in the upper NEADW to ~50% in the NEACW. East of Gibraltar, the observed decrease is ~30% in the WMDW. In contrast, no change was observed in the deepest waters (>3000 m) whose ventilation age exceeds 150 years, i.e. waters formed prior the industrial

era. These results corroborate the predicted decreasing Hg concentration trends in North Atlantic waters (e.g., Sunderland and Mason, 2007) as well as the expected decline in the Mediterranean Sea (Radjar et al., 2007). Our results suggest that regulations to reduce anthropogenic Hg emissions, starting with the 1970 US Clean Air Act to the more recent 2017 International Minamata Convention (UNEP, 2013), have had a positive effect on Hg contamination in parts of the marine environment. Abated anthropogenic Hg emissions decrease the Hg influx to the marine environment, its subsequent entrapment in the ocean's interior, and its availability for the formation of the toxic MeHg which biomagnifies through marine food webs. All other factors governing Hg methylation and bioaccumulation being equal, our results suggest that Hg bioavailability to Northeastern Atlantic and Western Mediterranean pelagic ecosystems, including edible fish species, is likely to have decreased between the two decades straddling the new millennium. A declining-trend in Hg levels in fish tissue in North American lakes over the period 1972-2016 has recently been demonstrated (Grieb et al., 2019), but in many cases the temporal trends in aquatic biota do not parallel changes in atmospheric concentrations and processes other than Hg concentrations must control MeHg bioaccumulation (Wang et al., 2019). Hence, more information must be gathered to elucidate these complex processes, especially in marine environments.

Declarations of interest: none.

Acknowledgments: This research has been funded by the "Programme Flux Océaniques" conducted by CNRS as the French part of the international JGOFS, and the Global Mercury Observation System (GMOS, N°265113

European Union project), and the European Research Council (ERC-2010-StG-20091028). Thanks are due to P. Morin and Y. Le Merrer for providing nutrient data, K. Bowman for providing the HgT values at Sta. 5 (GEOTRACES, GA-03 transect), and M. Vautour and A. Mucci for English editing.

References

Amos, H.M., Jacob, D.J., Streets, D.G., Sunderland, E.M., 2013. Legacy impacts of all-time anthropogenic emissions on the global mercury cycle. Global Biogeochem. Cy. 27, 410–421, doi:10.1002/gbc.20040.

Béthoux, J.-P., El Boukhary, M.S., Ruiz-Pino, D., Morin, P., Copin-Montégut, C., 2005. Nutrient, Oxygen and Carbon Ratios, CO_2 Sequestration and Anthropogenic Forcing in the Mediterranean Sea. In: A. Saliot ed. The Mediterranean Sea. Hdb. Env. Chem. Vol. 5, Part K, pp. 67–86, Springer Berlin / Heidelberg. doi:10.1007/b107144.

Bloom, N.S., Crecelius, E.A., 1983. Determination of Mercury in Seawater at Subnanogram per Liter Levels. Mar. Chem. 14, 49-55.

Blum, J.D., Popp, B.N., Drazen, J.C., Choy, A., Johnson, M.W., 2013. Methylmercury production below the mixed layer in the North Pacific Ocean. Nature Geosci. 6, 879–884.

Bowman, K.L., Hammerschmidt, C.R., Lamborg, C.H., Swarr, G., 2015. Mercury in the North Atlantic Ocean: The U.S. GEOTRACES zonal and meridional sections. Deep-Sea Res. II 116, 251–261.

Broecker, W.S., 1979. A revised estimate for the radiocarbon age of the North Atlantic deep water. J. Geophys. Res. 84, 3218–3226, doi.org/10.1029/JC084iC06p03218.

Carracedo Segade, L.I., Gilcoto, M., Mercier, H., Pérez, F.F., 2015. Quasi-synoptic transport, budgets and water mass transformation in the Azores–Gibraltar Strait region during summer 2009. Progr. Oceanogr. 130, 47–64.

Clarkson T.W., Magos L., 2006. The toxicology of mercury and its chemical compounds. Critical Review in Toxicology 36, 609–662.

Cole, A.S., Steffen, A., 2010. Trends in long-term gaseous mercury observations in the Arctic and effects of temperature and other atmospheric conditions. Atmos. Chem. Phys. 10, 4661−4672.

Cooke, C.A., Balcom, P.H., Biester, H., Wolfe, A.P., 2009. Over three millennia of mercury pollution in the Peruvian Andes, PNAS 106, 8830–8834.

Cossa, D., Courau, P., 1990. An international intercomparison exercise for total mercury in seawater. Appl. Organomet. Chem. 4, 49–54.

Cossa, D., Martin, J.M., K. Takayanagi, K., Sanjuan, J., 1997. The Distribution and Cycling of Mercury in the Western Mediterranean. Deep-Sea Res. II 44, 721–740.

Cossa, D., Elbaz-Poulichet, F., Nieto, J.M., 2001. Mercury in the Tinto-Odiel Estuarine System (Gulf of Cadiz, Spain): Sources and Dispersion. Aquat. Geochem. 7, 1–12.

Cossa, D., Cotté-Krief, M.H., Mason, R.P., Bretaudeau-Sanjuan, J., 2004. Total mercury in the water column near the shelf edge of the European continental margin. Mar. Chem. 90, 21–29.

Cossa, D., Averty, B., N. Pirrone, N., 2009. The origin of methylmercury in the open Mediterranean water column. Limnol. Oceanogr. 54, 837–844.

Cossa, D., Heimbürger, L-E., Lannuzel, D., Rintoul, S.R., Butler, E.C.V., Bowie, A.R., Averty, B., Watson, R.J., Remenyi T., 2011. Mercury in the Southern Ocean. Geochim. Cosmochim. Acta 75, 4037–4052.

Cossa, D., X. Durrieu de Madron, J. Schäfer, L. Lanceleur, S. Guédron, R. Buscail, B. Thomas, J.-J. Naudin. 2017. The open sea as the main source of methylmercury in the water column of the Gulf of Lions (Northwestern Mediterranean margin). Geochim. Cosmochim. Acta 199, 212-231.

Cossa, D., Heimbürger, L.E., Pérez, F.F., García-Ibáñez, M.I., Sonke, J.E., Planquette, H., Lherminier, P., Boutorh, J., Cheize, M., Menzel, J.L. Barraqueta, J.L., Shelley, R., Sarthou, G., 2018a. Mercury distribution and transport in the North Atlantic Ocean along the GEOTRACES-GA01 transect. Biogeosciences 15, 1–15.

Cossa, D., Durrieu de Madron, X., Schäfer, J., Guédron, S., Marusczak, N., Castelle, S., Naudin, J.-J., 2018b. Sources and exchanges of mercury in the waters of the Northwestern Mediterranean margin. Progr. Oceanogr. 163, 172–183, doi.org/10.1016/j.pocean.2017.05.002.

Cunningham, S.A., 2000. Circulation and volume flux of the North Atlantic using synoptic hydrographic data in a Bernoulli inverse. J. Mar. Res. 58, 1, 1–35.

Courau, P., 1983. Dosage du mercure minéral dissous. Chap. XIX, p. 227-249. In: Manuel des Analyses Chimiques en Milieu Marin. Aminot, A., Chaussepied, M. eds. CNEXO BNDO/ Documentation, Brest (France), ISBN 2-902721-10-2, 395 pp.

de Simone, F., Gencarelli, N., Hedgecock, I.M., Pirrone, N., 2016. A Modeling Comparison of Mercury Deposition from Current Anthropogenic Mercury Emission Inventories. Environ. Sci. Technol. 50, 5154−5162, doi:10.1021/acs.est.6b00691.

Doney, S.C., Jenkins, W.J., Bullister, J.L., 1997. A comparison of ocean tracer dating techniques on a meridional section in the eastern North Atlantic. Deep-Sea Res. I 44, 603-626.

Driscoll, C.T., Mason, R.P., H.M., Jacob, D.J., Pirrone, N., 2013. Mercury as a Global Pollutant: Sources, Pathways, and Effects. Environ. Sci. Technol. 47, 4967–4983, doi:10.1021/es305071v.

Elbaz-Poulichet, F., Dezileau, L., Freydier, R., Cossa, D., Sabatier, P., 2011. A 3500-year record of Hg and Pb contamination in a Mediterranean sedimentary archive (the Pierre Blanche Lagoon, France), Environ. Sci. Technol. 45, 8642–8647.

EPA (Environmental Protection Agency, US). 2002. Method 1631, Revision E: Mercury in water by oxidation, purge and trap, and cold vapor atomic fluorescence spectrometry, EPA-821-R-02-019, water.epa.gov/scitech/methods/cwa/metals/mercury.

Fitzgerald, W.F., Lamborg, C.H., 2003. Geochemistry of Mercury in the Environment. In: Treatise on Geochemistry, K. Turekian and H. Holland eds. Vol. 9, B.S. Lollar ed., Chap. 4. ISBN 0-08-044344-3. Elsevier, pp.107–148.

Fitzgerald, W.F., Lamborg, C.H., Hammerschmidt, C.R., 2007. Marine Biogeochemical Cycling of Mercury. Chem. Rev. 107, 641–62, doi:10.1021/cr050353m.

García-Ibáñez, M.I., Pardo, P.C., Carracedo, L.I., Mercier, E., Lherminier, P., Ríos, A.F., Pérez, F.F., 2015. Structure, transports and transformations of the water masses in the Atlantic Subpolar Gyre. Progr. Oceanogr., 135, 18-35, dx.doi.org/10.1016/j.pocean.2015.03.009.

García-Lafuente, J., Naranjo, C., Sammartino, S., Sánchez-Garrido, J.C., Delgado, J., 2017. The Mediterranean outflow in the Strait of Gibraltar and its connection with upstream conditions in the Alborán Sea. Ocean Sci. 13, 195–207, doi:10.5194/os-13-195-2017.

Gencarelli, C.N., De Simone, F., Hedgecock, I.M., et al., 2015. European and Mediterranean mercury modelling: Local and long-range contributions to the deposition flux. Atmos. Environ. 117, 162–168.

Gill, G.A., Fitzgerald, W.F., 1985. Mercury sampling of open ocean waters at the picomolar level, Deep-Sea Res. A 32, 287–297, doi.org/10.1016/0198-0149(85)90080-9.

Gregg, W.W., Conkright, M.E., Ginoux, P., O'Reilly, J.E., Casey, N.W., 2003. Ocean primary production and climate: Global decadal changes. Geophys. Res. Lett. 30, 15, 1809, doi:10.1029/2003GL016889.

Grieb, T.M., Fisher, N.S., Karimi, R., Levin, L., 2019. An assessment of temporal trends in mercury concentrations in fish. Ecotoxicology, doi.org/10.1007/s10646-019-02112-3.

Heimbürger, L.E., Lavigne, H., Migon, C., d'Ortenzio, F., Estournel, C., Coppola, L., Miquel, J.-C., 2013. Temporal variability of vertical export flux at the DYFAMED time-series station (Northwestern Mediterranean Sea). Progr. Oceanogr. 119, 59–67.

Hollweg, T.A., Gilmour, C.C., Mason, R.P., 2010. Mercury and methylmercury cycling in sediments of the mid-Atlantic continental shelf and slope. Limnol. Oceanogr. 55, 2703–2722.

Jensen, S., Jernelöv, A., 1969. Biological methylation of mercury in aquatic organisms. Nature 223, 753–754.

Lamborg, C.H., Hammerschmidt, C.R., Gill, G.A., Mason, R.P., Gichuki, S., 2012. An intercomparison of procedures for the determination of total mercury in seawater and recommendations regarding mercury speciation during GEOTRACES cruises. Limnol. Oceanogr. Meth. 10, 90–100, doi:10.4319/lom.2012.10.90.

Lamborg, C., Bowman, K., Hammerschmidt, C., Gilmour, C., Munson, K., Selin, N., Tseng, C.-M., 2014a. Mercury in the anthropocene ocean. Oceanography 27, 76–87, doi.org/1.5670/oceanog.2014.11.

Lamborg, C.H., Hammerschmidt, C.R., Bowman, K.L., Swarr, G.J., Munson, K.M., Ohnemus, D.C., Lam, P.J., Heimbürger, L.E., Rijkenberg, M.J.A., Saito, M.A., 2014b. A global ocean inventory of anthropogenic mercury based on water column measurements. Nature 512, 65–68.

Lamborg, C.H., Hammerschmidt, C.R., Bowman, K.L., 2016. An examination of the role of particles in oceanic mercury cycling. Phil. Trans. R. Soc. A 374: 20150297. http://dx.doi.org/10.1098/rsta.2015.0297

Macias, D., Garcia-Gorriz, E., Stips, A., 2018. Deep winter convection and phytoplankton dynamics in the NW Mediterranean Sea under present climate and future (horizon 2030) scenarios. Sci. Rep. 8, 6626. doi:10.1038/s41598-018-24965-0.

Mao, H., Talbot, R., 2012. Speciated mercury at marine, coastal, and inland sites in New England – Part 1: Temporal variability, Atmos. Chem. Phys. 12, 5099-5112, https://doi.org/10.5194/acp-12-5099-2012.

Marty, J.C., Chiavérini, J., 2010. Hydrological changes in the Ligurian Sea (NW Mediterranean, DYFAMED site) during 1995–2007 and biogeochemical consequences. Biogeosciences 7, 2117–2128.

Mason, R.P., Fitzgerald, W.F., 1990. Alkylmercury species in the Equatorial Pacific. Nature 347, 457–459.

Mason, R.P., Fitzgerald, W.F., 1993. The distribution and biogeochemistry cycling of mercury in the Equatorial Pacific Ocean. Deep-Sea Res. I 40, 1897–1924.

Mason, R.P., Choi, A.L., Fitzgerald, W.F., Hammerschmidt, C.R., Lamborg, C.H., Soerensen, A.L. Sunderland, E.M., 2012. Mercury biogeochemical cycling in the ocean and policy implications. Environ. Res. 119, 101–117.

Mason, R.P., Hammerschmidt, C.R., Lamborg, C.H., Bowman, K.L., Swarr, G.J., Shelley, R.U., 2017. The air-sea exchange of mercury in the low latitude Pacific and Atlantic Oceans. Deep-Sea Res. I 122, 17–28, doi.org/10.1016/j.dsr.2017.01.015.

McCartney, M.S., 1992. Recirculating components to the deep boundary current of the northern North Atlantic. Prog. Oceanogr. 29, 283– 383.

Millot, C., Candela, J., Fuda, J.-L., Tber, Y. 2006. Large warming and salinification of the Mediterranean outflow due to changes in its composition. Deep-Sea Res. I 53, 656–666, doi:10.1016/j.dsr.2005.12.017.

Minster, J.-F., Boulahdid, M., 1987. Redfield ratios along isopycnal surfaces – a complementary study. Deep-Sea Res. I 34, 1981–2003.

Monperrus, M., Tessier, E., Amouroux, D., Leynaert, A., Huonnic, P., Donard, O.F.X., 2007. Mercury methylation, demethylation and reduction rates in coastal and marine surface waters of the Mediterranean Sea. Mar. Chem. 10, 49–63.

Muntean, M, Janssens-Maenhout, G., Song, S.,. Selin, N.E., Olivier, J.G.J., Guizzardi, D. Mass, R., Dentener, F., 2014. Trend analysis from 1970 to 2008 and model evaluation of EDGARv4 global gridded anthropogenic mercury emissions. Sci. Total Environ. 494-495, 337–350. https://doi.org/10.1016/j.scitotenv.2014.06.014.

Outridge, P.M., Mason, R.P., Wang, F., Guerrero, S., Heimbürger, L-E., 2018. Updated global and oceanic mercury budgets for the United Nations Global Mercury Assessment 2018. Environ. Sci. Technol. 52, 11466-11477, doi:10.1021/acs.est.8b01246.

Parks, J.M., Johs, A., Podar, M., Bridou, R., Hurt, R.A., Smith, S. D., Tomanicek, S.J., Qian Y., Brown, S.D., Brandt, C.C., Palumbo, A.V., Smith, J.C., Wall, J.D., Elias, D.A., Liang, L., 2013. The genetic basis for bacterial mercury methylation. Science 339, 1332–1335.

Pérez, F.F., Fontela, M., García-Ibáñez, M.I., Mercier, H., Velo, A., Lherminier, P., Zunino, P., de la Paz, M., Alonso-Pérez, F., Guallart, E.F., Padin, X.A., 2018. Meridional overturning circulation conveys fast acidification to the deep Atlantic Ocean. Nature 554, 515–518, doi:10.1038/nature2549.

Pirrone, N., Cinnirella, S., Feng, X., Finkelman, R.B., Friedli, H.R., Leaner, J., Mason, R.P., Mukherjee, A.B., Stracher, G.B., Streets, D.G., Telmer, K., 2010. Global mercury emissions to the atmosphere from anthropogenic and natural sources. Atmos. Chem. and Phys. 10, 5951−5964.

Prestbo, E.M., Gay, D.A., 2009. Wet deposition of mercury in the US and Canada, 1996-2005: Results and analysis of the NADP mercury deposition network (MDN). Atmos. Environ. 43, 4223–4233.

Prieur, L., Sournia, A., 1994. "Almofront-1" (April–May 1991): an interdisciplinary study of the Almeria-Oran geostrophic front, SW Mediterranean Sea. J. Mar. Syst. 5, 187 –203.

Rajar, R., Cetina, M., Horvat, M., Zagar, D., 2007. Mass balance of mercury in the Mediterranean Sea. Mar. Chem. 107, 89−102.

Rhein, M., Fisher, J., Smethie, W.M., Smythe-Wright, D., Weiss, R.F., Mertens, C., Min, D.-H., Fleischmann, U., Putzka, A., 2002. Labrador Sea water: Pathways, CFC Inventory, and Formation Rates. J. Phys. Oceanogr. 32, 648–665.

Schneider, A., Tanhua, T., Roether, W., Steinfeldt, R., 2014. Changes in ventilation of the Mediterranean Sea during the past 25 year. Ocean Sci. 10, 1–16.

Semeniuk, K., and A. Dastoor. 2017. Development of a global ocean mercury model with a methylation cycle: Outstanding issues, Global Biogeochem. Cy. 31, 400–433, doi:10.1002/2016GB005452.

Sigman, D.M., Haug, G.H., 2006. The biological pump in the past. In: Treatise on Geochemistry, K. Turekian and H. Holland eds. Vol. 6, H. Elderfield ed., pp. 625. ISBN 0-08-043751-6. Elsevier, 2003., p.491-528.

Slemr, F., Brunke, E.G., Ebinghau,s R., Kuss, J., 2011. Worldwide trend of atmospheric mercury since 1995. Atmos. Chem. Phys. 11, 4779–4787.

Soerensen, A.L., Sunderland, E.M., Holmes, C.D., Skov, H., Christensen, J.H., Jacob, D.J., Strode, S., Mason, R.P., 2010. An Improved Global Model for Air-Sea Exchange of Mercury: High Concentrations over the North Atlantic. Environ. Sci. Technol. 44, 8574-8580.

Soerensen, A.L., Jacob, D.J., Streets, D.G., Witt, M.L.I., Ebinghaus, R., Mason, R.P., Andersson, M., Sunderland, E.M., 2012. Multi-decadal decline of mercury in the North Atlantic atmosphere explained by changing subsurface seawater concentrations. Geophy. Res. Lett. 39, 6 pages, L21810, doi:10.1029/2012GL053736.

Soerensen, A.L., Jacob, D.J., Schartup, A.T., Fisher, J.A., Lehnherr, I., St. Louis, V.L., Heimbürger, L.E., Sonke, J.E., Krabbenhoft, D.P., Sunderland, E.M., 2016. A Mass Budget for Mercury and Methylmercury in the Arctic Ocean. Global Biogeochem. Cy. 30 (4) (April): 560–575. Portico. doi:10.1002/2015gb005280.

Sonke, J.E., Heimburger, L.-E., Dommergue, A., 2013. Mercury biogeochemistry: paradigm shifts, outstanding issues and research needs. CR Geosci. 345, 213–222.

Sprovieri, F., Pirrone, N., Ebinghaus, R., Kock, H., Dommergue, A., 2010. A review of worldwide atmospheric mercury measurements. Atmos. Chem. Phys. 10, 8245–8265.

Streets, D.G., Zhang, Q., Wu, Y., 2009. Projections of global mercury emissions in 2050. Environ. Sci. Technol. 43, 2983−2988.

Sunderland, E.M., Mason, R.P., 2007. Human impacts on open ocean mercury concentrations. Global Biogeochem. Cy. 21, GB4022, 1–15. https://doi.org/10.1029/2006GB002876.

Tintoré, J., La Violette, P.E., Blade, I., Cruzado, A., 1988. A Study of an Intense Density Front in the Eastern Alboran Sea: The Almeria-Oran Front. J. Phys. Oceanogr. 18, 1384–1397.

Tsuchiya, M., Talley, L.D., McCartney, M.S., 1992. An eastern Atlantic section from Iceland southward across the equator. Deep-Sea Res. Part A 39, 1885–1917.

UNEP, 2013. Global Mercury Assessment 2013: Sources, Emissions, Releases and Environmental Transport. UNEP Chemicals Branch, Geneva, Switzerland. http://wedocs.unep.org/handle/20.500.11822/7984.

Van Geen, A., Boyle E.A., Moore, W.S., 1991. Trace metal enrichments in waters of the Gulf of Cádiz, Spain. Geochim. Cosmochim. Acta 55, 2173–2191.

Wang, F., Outridge, P.M., Feng, X., Meng, B., Heimbürger-Boavida, L.E., Mason, R.P., 2019. How closely do mercury trends in fish and other aquatic wildlife track those in the atmosphere? – Implications for evaluating the effectiveness of the Minamata Convention. Sci. Total Environ. 674, 58-70.

Weigelt, A., Ebinghaus, R., Manning, A.J., Derwent, R.G., Simmonds, P.G., Spain, T.G., Jennings, S.G., Slemr, F., 2014. Analysis and Interpretation of 18 years of mercury observations since 1996 at Mace Head, Ireland. Atmos. Environ. 100, 85–93.

Yoon, Y.-Y., Han, M.-H., Lee, J.-S., 1996. Distribution of Zn Concentrations in the Western Mediterranean Sea and its Influence on the North East Atlantic Ocean. Environ. Engin. Res. 2, 41–49.

Zhang, Y., Jaeglé, L., Thompson, L.A., 2014a. Natural biogeochemical cycle of mercury in a global three-dimensional ocean tracer model, Global Biogeochem. Cy. 28, 553–570, doi:10.1002/ 2014GB004814.

Zhang, Y., Jaeglé, L., Thompson, L.A., Streets, D.G., 2014b. Six centuries of changing oceanic mercury, Global Biogeochem. Cy. 28, 1251–1261, doi:10.1002/2014GB004939.

Zhang, Y., Jacob, D.J., Horowitz, H.M., Chen, L., Amos, H.M., Krabbenhoft, D.P., Slemr, F., St. Louis, V.L., Sunderland, E.M., 2016. Observed decrease in atmospheric mercury explained by global decline in anthropogenic emissions. PNAS 113, 526–531, www.pnas.org/cgi/doi/10.1073/pnas.1516312113.

Figure captions

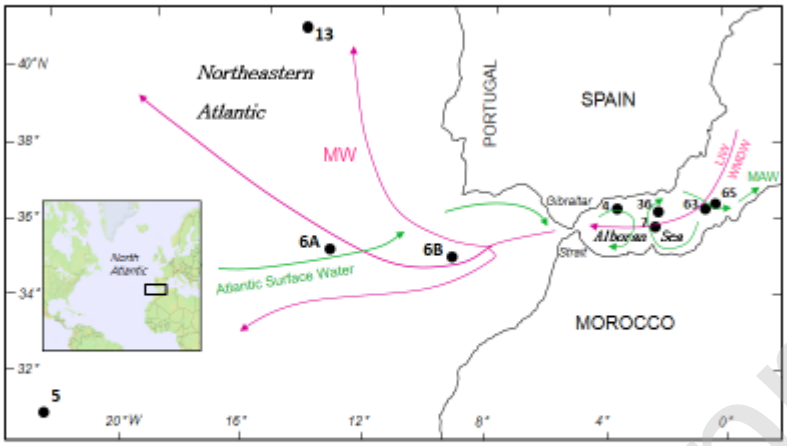

Fig. 1

Figure 1. Sampling locations within the North-eastern Atlantic Ocean and Western Mediterranean during the MEDALTANTE-II, ALMOFRONT-I and FENICE cruises. Sta. 6A on September 5, 1989 (35.6732°N; 13.1588°W, bottom depth 4460 m); Sta. 6B on August 18, 2012 (35.5137°N; 09.1532°W, bottom depth 3610 m); Sta. 36 on April 30, 1991 (36.2231°N; 2.5336°W, bottom 987 m); Sta. 63 on May 3, 1991 (36.2183°N; 1.0733°W, bottom 2601 m); Sta. 65 on 3 May, 1991 (36.3169°N; 0.5831°W, 2657 m); Sta. 4 on August 16, 2012 (36.4971°N; 4.0356°W, bottom 680 m) ; Sta. 7 on August 15, 2012 (35.9039°N; 2.6943°W, bottom 990 m). In addition, Sta. 5 (31°N; 22°W, bottom 5175 m) and Sta. 13 (41.3830°N; 13.8877°W, bottom 5350 m) were occupied during the GEOTRACES-GA03 (August 2010) and GA-01 (June 23, 2014), respectively. Arrows indicate main patterns of oceanic circulation: Atlantic surface waters entering the Mediterranean Sea through the Gibraltar Strait, Modified

Atlantic Water (MAW) at the surface in the Alboran Sea, and at depth: Levantine Intermediate Water (LIW), Western Mediterranean Deep Water (WMDW).

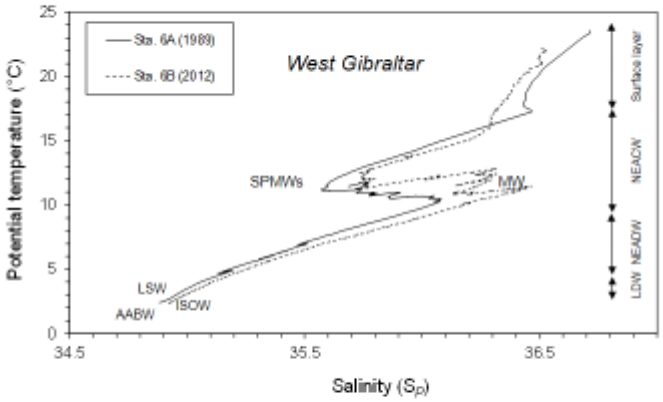

Fig. 2

Figure 2. Salinity-Temperature graphs in the water column West of Gibraltar at Stas. 6A and 6B during the MEDATLANTE-II and FENICE cruises. NEACW: North East Atlantic Central Water; NEADW: North East Atlantic Deep Water; LDW: Lower Deep Water; SPMWs: Subpolar Mode Waters; MW: Mediterranean Water; LSW: Labrador Sea Water; ISOW: Island Scotland Outflow Water; AABW: Antarctic Bottom Water.

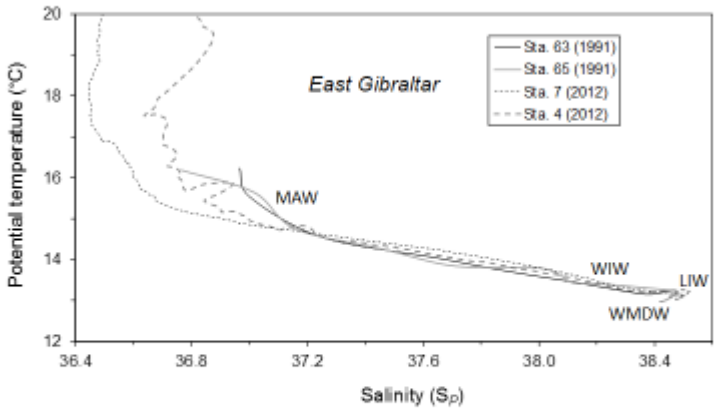

Fig. 3

Figure 3. Salinity-Temperature graphs in the water column East of Gibraltar at Stas. 63, 65, 4 and 7 during the ALMOFRONT-I and FENICE cruises. Modified Atlantic Water; WIW: Winter Intermediate Water; LIW: Levantine Intermediate Water; WMDW: Western Mediterranean Deep Water.

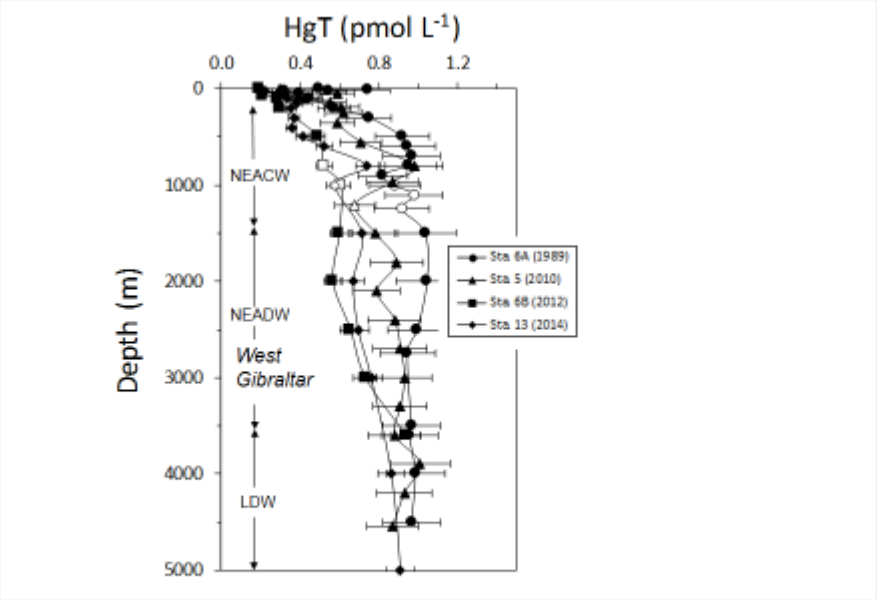

Fig. 4

Figure 4. Concentration profiles of total Hg (HgT) West of Gibraltar at Sta. 6A (FENICE cruise), Sta. 6B (MEDATLANTE-II cruise), Sta. 5 (31°N; 22°W, GEOTRACES GA-03 cruise), Sta. 13 (41°23'N; 13°53'W, GEOTRACES GA-01 cruise). Open marks correspond to salinity maxima due to the presence of the maximum proportion (≤ 25%) of Mediterranean waters (MW) along with the profile. NEACW: North East Atlantic Central Water; NEADW: North East Atlantic Deep Water; LDW: Lower Deep Water.

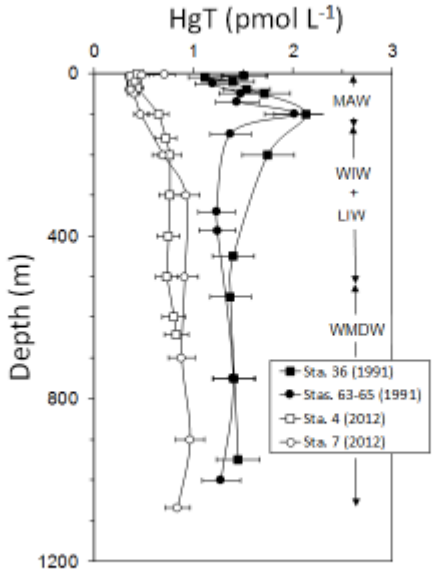

Fig. 5

Figure 5. Concentration profiles of total Hg (HgT) east of Gibraltar at Stas. 36, 63 and 65 (ALMOFRONT-I cruise), and Stas. 4 and 7 (FENICE cruise). MAW: Modified Atlantic Water; WIW: Winter Intermediate Water; LIW: Levantine Intermediate Water; WMDW: Western Mediterranean Deep Water.

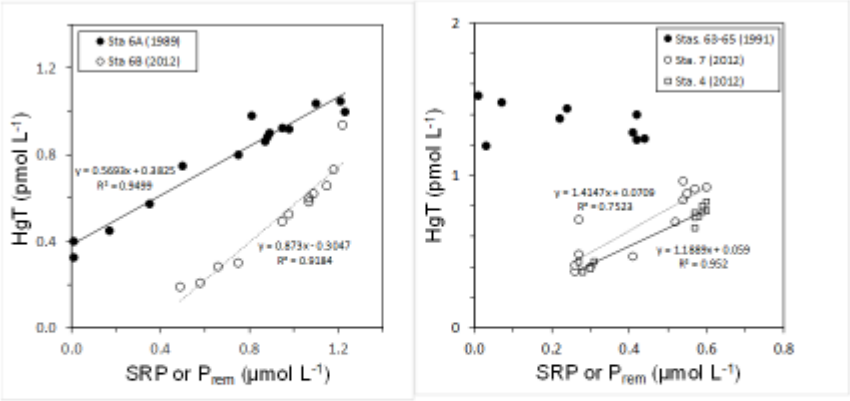

Fig. 6

Figure 6. Relationships between concentrations of total Hg (HgT) and soluble reactive phosphorus (SRP) or remineralized phosphorus (P_{rem}). (a) West of Gibraltar at Stas. 6A and 6B, (b) east of Gibraltar at Stas. 4 and 7.